

What can we learn from Raman spectra of nanopowders?

Andrey G. Yashenkin^{1,2}, Oleg I. Utesov^{1,2,3,*} and Sergei V. Koniakhin^{4,3†}

¹*Petersburg Nuclear Physics Institute, NRC "Kurchatov Institute", Orlova Roshcha, Gatchina 188300, Russia*

²*Department of Physics, St. Petersburg State University,
7/9 Universitetskaya nab., St. Petersburg 199034, Russia*

³*Nanotechnology Research and Education Centre of the Russian Academy of Sciences,
St. Petersburg Academic University, St. Petersburg 194021, Russia and*

⁴*Institute Pascal, PHOTON-N2, University Clermont Auvergne,
CNRS, 4 Avenue Blaise Pascal, 63178 Aubière Cedex, France*

(Dated: September 6, 2022)

The phenomenon of line broadening for optical vibrational eigenmodes in nanoparticles is incorporated into the microscopic theory of Raman scattering in nanopowders of nonpolar crystals. Particular broadening mechanism investigated in details is the phonon scattering by weak delta-correlated spatially randomized variations of atomic masses. Analytical calculations reveal parametrically different behavior of the linewidth in regimes of separated and overlapped levels. The dependence of linewidths on the particle mean size, shape, variance of the size distribution function, strength of disorder, as well as on phonon quantum numbers is determined for both regimes, and crossover scales for mean size and disorder strength are obtained. Analytical results are strongly supported by numerical calculations. The possibility to extract the aforementioned parameters (excluding quantum numbers) from experimental data on the Raman peak shape and position is demonstrated and illustrated with the use of concrete example.

Multifarious nanoparticles, assembled in ordered arrays of quantum dots, photonic crystals, etc.,¹ or existing in random formations of powders or liquid suspensions² are apparently the most intensively studied objects in modern chemistry and physics. Current close attention to these entities is fuelled by their possible plural scientific and industrial applications^{3–5}. Nonpolar nanocrystals, including diamond-like and semiconducting ones are definitely very promising candidates for technological utilizations^{6,7}. A great amount of experimental methods, namely X-ray diffraction, dynamical light scattering, atomic force microscopy, Raman spectroscopy, etc., are used in order to investigate and characterize these materials^{8–14}. The latter method is of our special interest because it is seen as a precise nondestructive instrument to observe the peculiarities of collective excitations in nanoparticles^{15–17}.

Reliable analysis of Raman peak shape and position would equip us with detailed information about the nanopowders. Finite-size quantization of the momentum in particles results in size-dependent shift of the peak as compared to the bulk material¹⁸. Also, the spectrum of vibrational modes that (after the broadening) form the peak depends on the shape of particles. In Refs.¹⁹ and²⁰ we developed two theories capable to evaluate Raman data more confidently and precisely than the previously used phonon confinement model (PCM)^{21–24}. Presently, the lion part of efforts of the community is devoted to incorporating fine effects into the PCM^{24–29} although alternative models are also proposed³⁰.

Our first theory (DMM-BPM) is built upon the physically well-grounded dynamical matrix method (DMM) of calculation of vibrational modes in a particle, with forthcoming treatment of the photon-phonon interaction induced polarization within the framework of the bond

polarization model (BPM)¹⁹. The resulting Raman spectra empirically broadened (the linewidth Γ is treated as a fitting parameter) and smeared with the use of the size distribution function constitute the main (and subsequent) Raman peaks observed experimentally.

The second theory (EKFG) treats the long wavelength optical phonon modes in a particle which principally contribute to the Raman peak within the effective medium approach replacing original problem by the solution of the Klein-Fock-Gordon equation with Dirichlet boundary conditions in the Euclidian space²⁰. Being supplemented by the continuous version of the BMP, after line broadening and peak smearing procedures this theory generates Raman peaks undistinguishable from those obtained by the DMM-BPM method.

Both these theories capture principal features of optical phonon spectra in nanoparticles, including (i) existence of “Raman active” (contributing to Raman peaks) and “Raman silent” (not contributing) eigenmodes and (ii) presence of the first triple-degenerate level supplying the majority (around 2/3) of the total spectral weight. This level is separated from the next one by the large gap tangibly exceeding typical inter-level distances in the rest of the spectrum. The latter forms (iii) several “bands”, each of them could be treated as a (quasi)continuum. (iv) The structure of these bands strongly depends on the particle shape. The theories successfully explain recent experimental data on nanodiamonds and semiconducting nanocrystals^{19,20}.

The disadvantage of both these approaches is the absence of a microscopic mechanism to provide the phonon line broadening. No microscopic explanation of this phenomenon currently exists in literature, as well (see, however, phenomenological analysis of experiments in Refs.^{31,32} and³³). Below we accomplish our theories^{19,20}

introducing disorder as the origin of a finite linewidth of phonon eigenmodes in nanoparticles.

We consider analytically weak delta-correlated randomness of atomic masses as a source of spatial disorder (another possible choice would be the variation of spring rigidities; we believe that it does not change our principal results). We observe that the linewidths of optical vibrational modes behave differently for separated and overlapped levels, the levels are capable to overlap due to their finite linewidths.

In the former case we applied independent levels approximation and self-consistent Born approximation in order to obtain specific dependence of the linewidth Γ on the particle size L and disorder strength S in the form $\Gamma \propto \sqrt{S}/L^{3/2}$, where the prefactor depends on the quantum number of the level n as well as on the shape of a particle parametrized by the effective faceting number p (elongated particles are not considered). The disorder strength S is the product of dimensionless impurity concentration c_{imp} and squared relative mean mass variation $\delta m/M$, providing $S = c_{imp}(\delta m/M)^2$.

In the latter case of overlapped levels we used the following trick: we consider first the bulk problem and then replace the q -dependence of the linewidth by the finite size quantization rule $q \rightarrow q_n(L, p)$ appropriate for this particle shape. Justification of the trick can be found in the body of this paper (see also Refs.^{34,35}). The linewidths obtained on this way are given by $\Gamma \propto S/L$, the prefactors are n and p depended, as well.

We investigate crossover scales between these regimes for particle size L and disorder strength S .

Accompanying analytical calculations by numerical modelling of the disordered Raman problem in nanoparticles, we found that numerics strongly supports our conclusions. Furthermore, we fitted experimental data of Ref.³⁶ with the use of our theory thus proving the capability of this approach to retrieve from the experiment such important characteristics of a nanopowder as the particle mean size L , the variance of the particle size distribution function σ , the strength of disorder S , and the effective faceting number p .

Details, extensions and generalizations of this research will be published elsewhere^{34,35}.

The starting point of our evaluation is the Hamiltonian of elastic medium which reads:

$$\mathcal{H} = \sum_j \frac{p_j^2}{2M_j} + 1/2 \sum_{ij} \mathcal{K}_{ij} (\mathbf{r}_i - \mathbf{r}_j)^2, \quad (1)$$

where the first sum describes the kinetic energy of atoms with masses M_j packed in a lattice. These atoms are connected by springs with rigidities \mathcal{K}_{ij} , the elastic energy (second sum) being proportional to the second power of a difference of atomic displacements from lattice sites \mathbf{r}_j . We incorporate disorder via the spatial variation of atomic masses M_j , with the mean value $M = \langle M_j \rangle$ and the mass variation having zero average $\langle \delta m_j \rangle = 0$ and delta-functional pairwise correlator $\langle \delta m_i \delta m_j \rangle / M^2 =$

$S \delta_{ij}$. Here $S = c_{imp}(\delta m/M)^2 \ll 1$ is the strength of disorder and c_{imp} is the dimensionless impurity concentration. Disorder enters Hamiltonian \mathcal{H} as follows:

$$\mathcal{H}_{imp} = - \sum_j \delta m_j \frac{p_j^2}{2M}, \quad (2)$$

Let $\{\Psi_n(\mathbf{R}_j)\}_{n=1}^{3N}$ be a set of normalized vibrational eigenmodes for the nanoparticle of given shape and size, where N is the number of atoms in a particle, n is the generalized quantum number, and ω_n are the corresponding eigenfrequencies. Then for a diamond-like crystal atomic displacements \mathbf{r}_j and momenta \mathbf{p}_j are given by

$$\begin{aligned} \mathbf{r}_j &= \frac{1}{\sqrt{2M}} \sum_n \frac{\Psi_n(\mathbf{R}_j)}{\sqrt{\omega_n}} (b_n + b_n^\dagger) \\ \mathbf{p}_j &= \frac{i\sqrt{M}}{\sqrt{2}} \sum_n \Psi_n(\mathbf{R}_j) \sqrt{\omega_n} (b_n^\dagger - b_n). \end{aligned} \quad (3)$$

Here b_n^\dagger (b_n) are bosonic creation (annihilation) operators written in the basis $\{\Psi_n(\mathbf{R}_j)\}$. Plugging Eqs. (3) into Eqs. (1) and (2) one gets Hamiltonian (1) in the form $\mathcal{H} = \mathcal{H}_0 + \mathcal{H}_{imp}$, where \mathcal{H}_0 represents free phonons

$$\mathcal{H}_0 = \sum_n \omega_n (b_n^\dagger b_n + 1/2) \quad (4)$$

and \mathcal{H}_{imp} describes the phonon-impurity interaction

$$\begin{aligned} \mathcal{H}_{imp} &= \frac{1}{4} \sum_{j,n,n'} \frac{\delta m_j}{M} \Psi_n(\mathbf{R}_j) \cdot \Psi_{n'}(\mathbf{R}_j) \\ &\quad \sqrt{\omega_n \omega_{n'}} (b_n^\dagger - b_n) (b_{n'}^\dagger - b_{n'}). \end{aligned} \quad (5)$$

Defining the phonon propagator $D_n(\omega)$ as the Green's function for operators $\phi_n = i(b_n^\dagger - b_n)$ we get:

$$D_n(\omega) = \frac{2\omega_n}{\omega^2 - \omega_n^2 - 2\omega_n \Pi_n(\omega)}, \quad (6)$$

where the interaction-induced self energy term $\Pi_n(\omega)$ after impurity averaging obtains the form:

$$\Pi_n(\omega) = \frac{S\omega_n}{16} \sum_{j,n'} [\Psi_n(\mathbf{R}_j) \cdot \Psi_{n'}(\mathbf{R}_j)]^2 \omega_{n'} D_{n'}(\omega). \quad (7)$$

Eq. (7) allows to evaluate the phonon linewidth for separated levels. We shall use the self-consistent Born approximation keeping the phonon self-energy $\Pi_{n'}(\omega)$ on the r.h.s. of Eq. (7) nonzero (otherwise, $\text{Im } \Pi_n(\omega) = 0$). When the levels are separated, the main contribution to this equation comes from the term with $n' = n$. It yields:

$$\Pi_n(\omega) = \frac{\omega^2 - \omega_n^2 - \sqrt{(\omega^2 - \omega_n^2)^2 - \frac{16c^2(n,p)S\omega_n^4}{N}}}{4\omega_n}, \quad (8)$$

where $c^2(n,p) = N \sum_j [\Psi_n(\mathbf{R}_j)]^4 / 16$.

When the square root in Eq. (8) is imaginary it determines the well-known semi-circle law for the density

of states³⁷. Using the on-shell approximation $\omega = \omega_n$ in Eq. (8) we obtain the phonon linewidth in the form

$$\Gamma(L, S, n, p) = \omega_n C(n, p) \sqrt{S} \left(\frac{a}{L} \right)^{3/2}. \quad (9)$$

Here a is the lattice parameter, $C(n, p) = c(n, p) \sqrt{P^3(p)/2}$, and $P(p)$ is the shape dependent multiplier which converts the linear size of a particle with faceting number p (for cubic particles it is the cube edge) into the diameter of a sphere with the same amount of atoms. The factor $C(n, p)$ specific for any particle shape could be determined numerically.

Eq. (9) constitute our first principal result. It reveals unusual dependence of a phonon linewidth on the particle size, $\Gamma \sim L^{-3/2}$, disorder strength, $\Gamma \sim \sqrt{S}$, as well as on quantum number n and particle shape p via the factor $C(n, p)$ which this quantity demonstrates in the regime of separated levels.

The approach we utilize for separated phonon levels is very similar to the self-consistent theory of strongly disordered electrons³⁸ as well as to the theory of disordered electrons in high magnetic fields^{37,39}.

Now we switch to the case of overlapped levels arising with the growth of L and/or S . In order to proceed with this regime on the most economical way we shall use the following trick. Assuming that the basis of plane waves

$$\Psi_n(\mathbf{R}_j) = \frac{\mathbf{P}_q}{\sqrt{N}} e^{i\mathbf{q}\mathbf{R}_j} \quad (10)$$

properly captures the main features of the one of overlapped (and therefore extended) eigenmodes we consider first the bulk problem. Then we replace the q -dependence in final formulas by the finite size quantization rule peculiar for this particular particle shape, $q \rightarrow q_n(L, p)$. Here \mathbf{P}_q is the phonon polarization and $q_n(L, p)$ has the meaning of the discrete phonon quasimomentum. This approach is justified, in particular, by our numerical calculations (see below).

Repeating the derivation made above for the basis of plane waves one arrives to the phonon propagator

$$D(\omega, \mathbf{q}) = \frac{2\omega_{\mathbf{q}}}{\omega^2 - \omega_{\mathbf{q}}^2 - 2\omega_{\mathbf{q}}\Pi_{\mathbf{q}}(\omega)}. \quad (11)$$

with the self energy given by

$$\Pi_{\mathbf{q}}(\omega) = \frac{S\omega_{\mathbf{q}}}{16N} \sum_{\mathbf{k}} \omega_{\mathbf{k}} D_0(\omega, \mathbf{k}). \quad (12)$$

It is sufficient to take the phonon Green's function on the r.h.s. of Eq. (12) in the bare form, $-2\omega_{\mathbf{q}}\Pi_{\mathbf{q}}(\omega) \rightarrow i\delta$.

Dispersion of long wavelength optical phonons mainly contributing to Raman spectra reads:

$$\omega_{\mathbf{q}} = \omega_0 - \alpha q^2 = \omega_0 [1 - F(qa)^2], \quad (13)$$

where we introduced the dimensionless spectral flatness parameter F (for diamond, $F \approx 0.008$). The spectrum of finite-size particles is given by $\omega_n = \omega_0 - \alpha q_n^2$.

Evaluating Eq. (12) at $\omega \sim \omega_{\mathbf{q}}$ we get:

$$\Pi_{\mathbf{q}}(\omega) = -\frac{Sa^3\omega_{\mathbf{q}}}{64\pi\alpha^{3/2}} \omega \sqrt{\omega - \omega_0}, \quad (14)$$

where we absorbed into ω_0 the constant contribution to $\text{Re}\Pi_{\mathbf{q}}(\omega)$ stemming from the upper limit of integration in Eq. (12). Sharp nonanalytic frequency dependence of this self energy came from van Hove singularity in the density of states of intermediate phonons scattered by disorder. It leads to strong asymmetry of the phonon line shape near its maximum³⁴. Ignoring this asymmetry in the on-shell approximation $\omega = \omega_{\mathbf{q}}$ one finds:

$$\Gamma_{\mathbf{q}} = \omega_{\mathbf{q}} \frac{S}{32\pi F} (qa). \quad (15)$$

Applying to Eq. (15) the finite size quantization rule $q \rightarrow q_n(L, p)$ one finally obtains (cf. Ref.³¹):

$$\Gamma(L, S, n, p) = \omega_n C'(n, p) S \frac{a}{L}. \quad (16)$$

Here $C'(n, p) = c'(n, p)/32F$ is the coefficient containing strong dependence on the quantum number n via the factor $c'(n, p)$ to be determined numerically for any specific particle shape p . With increasing the quantum number the spectral linewidth increases, as well. In particular, for a cubic particle we have

$$\frac{\Gamma(L, S, \mathbf{n}, 6)}{\Gamma(L, S, \mathbf{1}, 6)} = \frac{|\mathbf{n}|}{\sqrt{3}}, \quad (17)$$

where $\mathbf{n} = (n_x, n_y, n_z)$ is the multicomponent quantum number describing size quantization in the cubic box and $\mathbf{1} = (1, 1, 1)$.

Eq. (17) constitute our second main result. It reveals that the linewidths of overlapped and separated levels are qualitatively different. In particular, we observe $\Gamma \sim 1/L$ instead of $\Gamma \sim 1/L^{3/2}$ and $\Gamma \sim S$ instead of $\Gamma \sim \sqrt{S}$.

Both above evaluations have been performed for non-degenerate spectral lines. One could easily show that the difference for degenerate levels occurs only in numerical prefactors which could be calculated (either analytically or numerically) for any specific particle shape (for details, see Refs.^{34,35}).

Let us estimate the characteristic particle size for the crossover from separated to overlapped regime of behavior. Neglecting numerical coefficients different for various particle shapes and quantum numbers we obtain:

$$\mathcal{L}_c \sim \frac{a}{S}. \quad (18)$$

Notice that the linewidth reaches the interlevel distance (thus providing the overlapped regime) on the same spatial scale \mathcal{L}_c . In general terms, it is the scale for the phonon lifetime $1/\Gamma$ to coincide with the time for phonon to traverse throughout the nanoparticle ballistically (cf. with the Thouless time in the diffusive regime of disordered electrons, see⁴⁰).

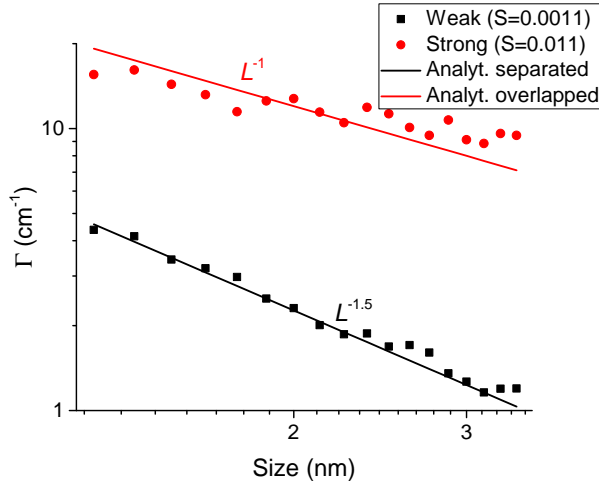


FIG. 1. Phonon linewidth Γ plotted as a function of the mean particle size L for two disorder strengths $S = 0.0011$ (black squares) and $S = 0.011$ (red dots). The range of L shown in this Figure corresponds to the regime of separated levels in the former case and to the regime of overlapped levels in the latter one. The lines represent predictions of the theory.

When the size of a particle is fixed, one can introduce the characteristic crossover scale of disorder dividing separated and overlapped regimes:

$$S_c \sim \frac{a}{L}. \quad (19)$$

We support our analytical calculations by proper numerics. In numerical studies we employ exact diagonalization of the dynamical matrix with atomic masses distributed according to the Gaussian law around the mean value M . The eigenmodes $|\varepsilon\rangle$ obtained in that way are utilized when calculating the broadening for the n -th mode of a pure particle. The averaging over disorder configurations is realized with the use of the spectral weight

$$\overline{\delta(\omega - \varepsilon)|\langle n|\varepsilon\rangle|^2}. \quad (20)$$

Here the overline stands for averaging. Then we fit the spectral lines by Lorentzians. In the averaging procedure we utilized several hundreds configurations for each particle size/disorder strength.

In Fig. 1 one can find the comparison of our numerical simulations and analytical calculations of the phonon linewidth drawn as a function of particle size in both regimes of separated and overlapped levels whereas Fig. 2 demonstrates the linewidth dependence on the disorder strength (including crossover between the regimes). We would like to emphasize very good agreement of our analytics and numerics including numerical prefactors, functional dependencies and crossover scales visible in these two Figures.

The theory of phonon line broadening developed in this paper accomplishes more general approach of Refs.¹⁹

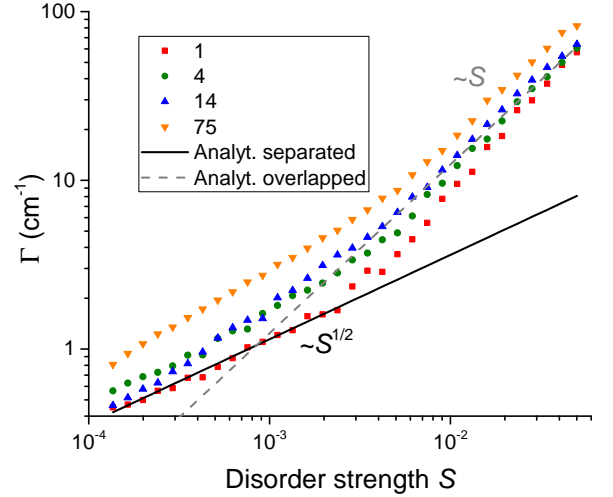


FIG. 2. Phonon linewidth Γ plotted as a function of disorder strength S for phonon eigenmodes ($n = 1, 4, 14, 75$) of a spherical 3 nm nanodiamond. Solid and dashed lines show theoretical predictions for the first mode in separated and overlapped regimes, respectively. Both functional dependencies and crossovers are clearly seen. Evidently, the highest phonon modes in the regime of overlapped levels have higher linewidths (see, e.g., Eqs. (15) and (17)). In the regime of separated levels one should sum up the coefficient $C(n, p)$ in Eq. (9) over the degeneracy and n dependence of the linewidth becomes more complicated.

and²⁰ providing us with the microscopic mechanism of the line broadening which includes shape and quantum number dependent factors. It yields the possibility to build up the regular method of analyzing the Raman spectra of nanopowders of nonpolar crystals more confidently and precisely than the previously used ones. This method allows to extract at least four parameters from the Raman peak shape and position, namely (i) the mean particle size in a powder L , (ii) the variance of the size distribution function σ , (iii) the disorder strength parameter S , and, hopefully, (iv) particle shape parameterized by the effective faceting number p . The thorough analysis of asymmetry of the Raman peak including the fast decay of its right shoulder due to asymmetry of the linewidth of the first phonon line and the shape-dependent long living left shoulder of the peak originated from levels forming the first (and possibly, subsequent) Raman active bands should play the crucial role in this approach. In present paper we undertake the simplified version of such analysis re-examining the experimental data of Ref.³⁶ with the use of EFKG method and utilizing our approach for phonon linewidths in the regime of overlapped levels (16), see Fig. 3. As it is shown in the inset we take five different particles shapes, namely sphere, truncated octahedron, dodecahedron, octahedron, and cube. We observe that the log-normal distribution function fits the experiment much better than the Gaussian. Best fit provides the fol-

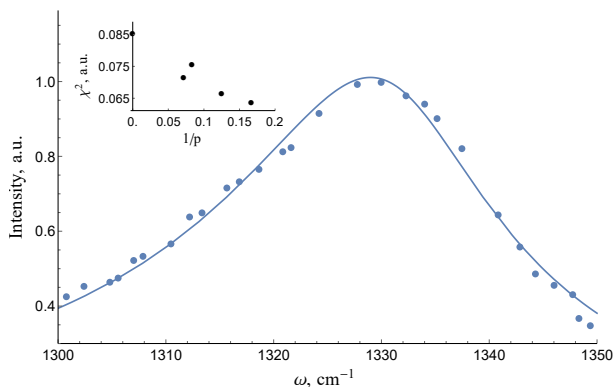


FIG. 3. EKFG model²⁰ fit for the experimental Raman spectrum³⁶ of a diamond nanopowder, the levels supposed to be overlapped. Solid blue line corresponds to the spectrum theoretically calculated for the log-normal distribution of cubic particles with $L \approx 2.64$ nm, $\sigma \approx 1.00$ nm, and $S \approx 0.03$. Inset shows χ^2 for the best fits obtained for spheres ($p = \infty$), truncated octahedra ($p = 14$), dodecahedra ($p = 12$), octahedra ($p = 8$), and cubes ($p = 6$).

lowing reliable values for four parameters: $L \approx 2.64$ nm, $\sigma \approx 1.00$ nm, $S \approx 0.03$, and $p = 6$, where L and σ are extracted from parameters of the log-normal distribution function. Notice that the octahedron ($p = 8$) yields χ^2 just a little bit larger than the cube. The possibility to perform such analysis is the third principal result of this paper. We also believe that more accurate Raman data and/or more accurate microscopic DMM-BPM method will allow determining the particle shape even more confidently.

Our treatment above dealt with elastic processes of phonon scattering by disorder, and, therefore, with Raman spectra at relatively low temperatures. At the same time, it is very interesting to investigate this issue at

arbitrary temperatures, when the inelastic processes of phonon scattering by each other could modify the situation. Here we just mention quite intriguing possibility to observe the localization-delocalization temperature crossover induced by many-body localization effects predicted in Refs.^{41,42} for the electron counterpart (interacting electrons in a quantum dot) of our problem.

To conclude, we investigated the elastic impurity-induced broadening of the linewidths of vibrational eigenmodes in nanopowders of nonpolar crystals and incorporated this issue into more complex problem of Raman peak evaluation in these materials. The disorder is chosen in the form of a weak delta-correlated (Born-like) spatial variation of atomic masses. Our analytical calculations demonstrate that the linewidths are essentially different for separated and overlapped phonon levels. In the latter case they reveal the linear dependence on the impurity strength S ; also, they are inversely proportional to the particle size L , providing $\Gamma \propto S/L$. In the former case they behave as $\Gamma \propto \sqrt{S}/L^{3/2}$. The prefactors are found to be specifically shape and quantum number dependent. The crossover spatial scale between these two regimes is found to be equal to the one for the elastic phonon lifetime Γ^{-1} to coincide with the time of ballistic traversing by phonon throughout the particle. These analytical results are strongly supported by our numerics. We also demonstrated that our theory of Raman peak shape and position allows to extract confidently from Raman data four important microscopic parameters such as the particle mean size, the variance of the particle size distribution function, the strength of intrinsic disorder, and the effective faceting number parameterizing the particle shape.

The authors are thankful to Igor Gornyi for valuable comments. This work is supported by the Russian Science Foundation (Grant No. 19-72-00031).

* utiosov@gmail.com

† kon@mail.ioffe.ru

¹ J. Roh, Y.-S. Park, J. Lim, and V. I. Klimov, *Nature Communications* **11**, 1 (2020).

² P. Geiregat, D. Van Thourhout, and Z. Hens, *NPG Asia Materials* **11**, 1 (2019).

³ M. Veldhorst, J. Hwang, C. Yang, A. Leenstra, B. de Ronde, J. Dehollain, J. Muhonen, F. Hudson, K. Itoh, A. Morello, *et al.*, *Nature nanotechnology* **9**, 981 (2014).

⁴ S. V. Kidalov and F. M. Shakhov, *Materials* **2**, 2467 (2009).

⁵ Y. Xia, H. Yang, and C. T. Campbell, “Nanoparticles for catalysis,” (2013).

⁶ K. D. Behler, A. Stravato, V. Mochalin, G. Korneva, G. Yushin, and Y. Gogotsi, *ACS nano* **3**, 363 (2009).

⁷ V. Pichot, M. Guerchoux, O. Muller, M. Guillevis, P. Fioux, L. Merlat, and D. Spitzer, *Diamond and Related Materials* **95**, 55 (2019).

⁸ R. Pecora, *Journal of nanoparticle research* **2**, 123 (2000).

⁹ B. Chu, *Laser light scattering: basic principles and practice* (Courier Corporation, 2007).

¹⁰ S. Mourdikoudis, R. M. Pallares, and N. T. Thanh, *Nanoscale* **10**, 12871 (2018).

¹¹ S. Koniakhin, I. Eliseev, I. Terterov, A. Shvidchenko, E. Eidelman, and M. Dubina, *Microfluidics and Nanofluidics* **18**, 1189 (2015).

¹² S. Koniakhin, N. Besedina, D. Kirilenko, A. Shvidchenko, and E. Eidelman, *Superlattices and Microstructures* **113**, 204 (2018).

¹³ P. A. Hassan, S. Rana, and G. Verma, *Langmuir* **31**, 3 (2015).

¹⁴ D. Segets, *KONA Powder and Particle Journal*, 2016012 (2016).

¹⁵ M. Cardona and R. Merlin, in *Light Scattering in Solid IX* (Springer, 2006) pp. 1–14.

¹⁶ A. C. Ferrari and J. Robertson, *Philosophical Transactions of the Royal Society of London. Series A: Mathematical, Physical and Engineering Sciences* **362**, 2477 (2004).

- ¹⁷ C. S. Kumar, *Raman spectroscopy for nanomaterials characterization* (Springer Science & Business Media, 2012).
- ¹⁸ A. Meilakhs and S. Koniakhin, *Superlattices and Microstructures* **110**, 319 (2017).
- ¹⁹ S. V. Koniakhin, O. I. Utesov, I. N. Terterov, A. V. Siklitskaya, A. G. Yashenkin, and D. Solnyshkov, *The Journal of Physical Chemistry C* **122**, 19219 (2018).
- ²⁰ O. I. Utesov, A. G. Yashenkin, and S. V. Koniakhin, *The Journal of Physical Chemistry C* **122**, 22738 (2018).
- ²¹ H. Richter, Z. Wang, and L. Ley, *Solid State Communications* **39**, 625 (1981).
- ²² I. Campbell and P. M. Fauchet, *Solid State Communications* **58**, 739 (1986).
- ²³ K. W. Adu, H. Gutierrez, U. Kim, G. Sumanasekera, and P. Eklund, *Nano letters* **5**, 409 (2005).
- ²⁴ G. Faraci, S. Gibilisco, P. Russo, A. R. Pennisi, and S. La Rosa, *Physical Review B* **73**, 033307 (2006).
- ²⁵ S. Osswald, V. Mochalin, M. Havel, G. Yushin, and Y. Gogotsi, *Physical Review B* **80**, 075419 (2009).
- ²⁶ V. I. Korepanov and H.-o. Hamaguchi, *Journal of Raman Spectroscopy* **48**, 842 (2017).
- ²⁷ V. I. Korepanov, H. o Hamaguchi, E. Osawa, V. Ermolenkov, I. K. Lednev, B. J. Etzold, O. Levinson, B. Zousman, C. P. Epperla, and H.-C. Chang, *Carbon* **121**, 322 (2017).
- ²⁸ J. Zi, K. Zhang, and X. Xie, *Physical Review B* **55**, 9263 (1997).
- ²⁹ W. Ke, X. Feng, and Y. Huang, *Journal of Applied Physics* **109**, 083526 (2011).
- ³⁰ Y. Gao and P. Yin, *Diamond and Related Materials* **99**, 107524 (2019).
- ³¹ M. Yoshikawa, Y. Mori, M. Maegawa, G. Katagiri, H. Ishida, and A. Ishitani, *Applied Physics Letters* **62**, 3114 (1993).
- ³² M. Yoshikawa, Y. Mori, H. Obata, M. Maegawa, G. Katagiri, H. Ishida, and A. Ishitani, *Applied Physics Letters* **67**, 694 (1995).
- ³³ M. Chaigneau, G. Picardi, H. A. Girard, J.-C. Arnault, and R. Ossikovski, *Journal of Nanoparticle Research* **14**, 955 (2012).
- ³⁴ O. I. Utesov, A. G. Yashenkin, and S. V. Koniakhin, unpublished.
- ³⁵ S. V. Koniakhin, O. I. Utesov, and A. G. Yashenkin, unpublished.
- ³⁶ O. A. Shenderova, I. I. Vlasov, S. Turner, G. Van Tendeloo, S. B. Orlinskii, A. A. Shiryaev, A. A. Khomich, S. N. Sulyanov, F. Jelezko, and J. Wrachtrup, *The Journal of Physical Chemistry C* **115**, 14014 (2011).
- ³⁷ T. Ando and Y. Uemura, *Journal of the Physical Society of Japan* **36**, 959 (1974).
- ³⁸ H. Haug and A.-P. Jauho, *Quantum kinetics in transport and optics of semiconductors*, Vol. 2 (Springer, 2008).
- ³⁹ M. Stone, *Quantum Hall Effect* (World Scientific, 1992).
- ⁴⁰ J. T. Edwards and D. J. Thouless, *Journal of Physics C: Solid State Physics* **5**, 807 (1972).
- ⁴¹ B. L. Altshuler, Y. Gefen, A. Kamenev, and L. S. Levitov, *Phys. Rev. Lett.* **78**, 2803 (1997).
- ⁴² I. V. Gornyi, A. D. Mirlin, D. G. Polyakov, and A. L. Burin, *Annalen der Physik* **529**, 1600360 (2017).